Interannual, probabilistic prediction of water resources over Europe following the heatwave and drought 2018

Carl Hartick[1,2,*], Carina Furusho-Percot[1,2], Klaus Goergen[1,2], and Stefan Kollet[1,2]

[1]Agrosphere (IBG-3), Research Centre Jülich GmbH, Jülich, Germany.

[2]Centre for High Performance Scientific Computing in Terrestrial Systems, Geoverbund ABC/J.

*Corresponding author: Carl Hartick (c.hartick@fz-juelich.de)

Key Points:

- Terrestrial systems modeling with the Terrestrial System Modeling Platform affords interannual probabilistic water resources predictions.
- The probability of an anomalously dry water year 2018/19 is high.
- The current trajectory suggests another extreme drought in late 2019.

Abstract

The year 2018 was one of the hottest and driest years in Europe having a large impact on agriculture, ecosystems and society. The associated drought in central and northern Europe underpins the need for water resources predictions at the seasonal to interannual time scale. In this study, we propose a probabilistic, terrestrial prediction system including water resources utilizing the Terrestrial Systems Modeling Platform, TSMP. Based on an existing climatology from 1996 to 2018, a probabilistic prediction for the water year 2018/19 was performed accounting for atmospheric uncertainty in an ensemble approach. The results show that the water year 2017/18 is an outlier with respect to dry conditions considering all available years of the climatology. The prediction shows that, on average, the water deficit will not be alleviated until the end of 2019 and that there is a higher probability for anomalously dry conditions. However, the current trajectory obtained from a simulation applying recent atmospheric reanalysis data is located in the dry tail of the ensemble potentially indicating a continuation of a severe drought in future.

1 Introduction

At the seasonal time scale and beyond, droughts associated with heat waves are difficult to predict, mainly because of uncertainty related to the atmospheric forcing (Miralles et al., 2019). However, the hypothesis is that memory effects related to slow dynamics of the groundwater-soil water-vegetation (GSV) system render the prediction challenge an initial value problem, which may lead to predictive skill potentially over extended periods (Dirmeyer, 2000). Here, the major assumption is that memory effects including interactions of the GSV system with the atmospheric forcing are correctly simulated in the forward model.

In recent years there have been many efforts to establish a reliable seasonal forecasting system applying various approaches. First, there is the possibility of using statistical tools e.g. linear stochastic models (e.g. Mishra and Desai, 2005), Bayesian frameworks (e.g. Madadgar and Moradkhani, 2013) or the collection and transformation of multiple datasets (e.g Hao et al., 2015). These approaches rely on drought indices derived from as much observational data as possible to derive probability density functions. Then there is the possibility to use climate models with a dynamical core, e.g. Yuan et al. (2013) and Yuan and Wood (2013). Because predictions with climate models alone generally do not lead to satisfactory results, there are recent studies that combine models with observational data using machine learning methods (Rhee and Im, 2017; Hosseini-Moghari and Araghinejad, 2015). Furthermore, there has been success with an experimental combination of hydrological modeling and regional climate forecasts in the Sub-Sahara region (Sheffield et al., 2013).

The importance of soil moisture and groundwater in the occurrence of extreme temperature events and droughts has been shown previously (e.g., Seneviratne et al., 2010; Hirschi et al., 2011). However, at the continental scale, weather forecast or climate models do not provide the whole water cycle and strongly simplify the GVS system generally neglecting groundwater dynamics. While hydrological models seem an alternative, at the continental scale, the groundwater compartment and coupling with the soil water are also simplified (Zink et al., 2016), which may affect adversely the simulation of memory effects (Lo & Famiglietti, 2010). Additionally, in hydrologic modeling, potential impacts of the subsurface and land surface on atmospheric processes affecting precipitation are not taken into account.

Thus, in order to relax simplifying assumptions, we propose the application of an integrated terrestrial systems modeling approach for water resources and drought prediction. In this study, integrated terrestrial modeling refers to the representation of the complete terrestrial hydrologic and energy cycle from groundwater across the land surface into the atmosphere. In the recent past, considerable advancements have been achieved since the early work of e.g., York et al. (2002) and Maxwell et al. (2007) to couple subsurface, land surface and atmospheric models to close the terrestrial cycles in models and provide physically consistent states and fluxes throughout the terrestrial system. At the continental scale, which is of interest in this study, e.g. Miguez-Macho and Fan (2012) and Walco et al. (2000) applied groundwater parameterizations and simulated the terrestrial cycle over the Amazon and also globally at relatively coarse spatial resolutions. Keune et al. (2016) used the Terrestrial Systems Modeling Platform (TSMP) including a 3D variably saturated groundwater representation in a continuum approach to show that surface-atmosphere feedbacks are well-captured and that groundwater actually mitigated the 2003 heatwave over Europe. Later Keune et al. (2018) showed that human water use related to groundwater abstraction and irrigation may systematically change the distribution of water resources due to local and non-local subsurface-land surface-atmosphere feedbacks.

In this study, we applied TSMP over the European continent in predictive mode to assess the evolution of water resources in the water year 2018/19 (September - August), the year after the record-breaking drought 2018, focusing especially on the representation of atmospheric uncertainty via ensemble simulations. The analyses concentrated on the Mid-European region and included anomalies of atmospheric and hydrologic variables based on a previously generated climatology. Additionally, we addressed the question whether the 2018 drought interacts with the atmosphere and potentially reduces precipitation amounts in the water year 2018/19 causing a positive drought feedback.

2 Methods

In the following, we briefly describe the relevant components of the integrated terrestrial systems model applied in this study, the experimental setup of the probabilistic prediction system, and the analyses of the anomalies and interactions with the atmosphere.

2.1 The Terrestrial Systems Modeling Platform (TSMP)

TSMP (Gasper et al., 2014; Shrestha et al., 2014) closes the terrestrial water and energy cycle from groundwater across the land surface into the atmosphere coupling the atmospheric model COSMO 5.1 with the land surface model CLM3.5 and the groundwater model ParFlow 3.2 via the Ocean Atmosphere Sea Ice Soil Model Coupling Toolkit (OASIS3-MCT). Below, we provide only a brief overview of TSMP; the interested reader is referred to Shrestha et al., 2014 and Gasper et al., 2014.

The non-hydrostatic model COSMO has been developed by a consortium of weather services under the leadership of the German Weather Service (Baldauf et al., 2011). With different configurations COSMO can serve as an operational weather forecast model or for regional scale climate simulations. COSMO solves the primitive Euler-equations and includes multiple types of precipitation, radiation and a 2.5 turbulence closure. It parametrizes shallow convection, energy and momentum transfer with the surface.

The Community Land Model (CLM3.5) consists of the shallow soil, snow layers, land cover, vegetation and handles the interaction with the atmosphere (Oleson et al., 2004, 2008). To accomplish this CLM3.5 parameterizes hydrologic, biologic and radiation processes, such as evapotranspiration, sensible and ground heat. In TSMP, CLM3.5 supplies COSMO with the boundary condition of surface albedos, energy fluxes, evapotranspiration, root-water uptake and surface stresses. The land cover is described by sixteen different plant functional types (PFTs). In TSMP, the hydrologic component of CLM3.5 is completely replaced by ParFlow.

The hydrological model ParFlow (Jones and Woodward, 2001; Ashby and Falgout, 1996; Kollet and Maxwell, 2006; Maxwell, 2013) solves the 3D Richards equation with a Newton-Krylov solver to model integrated variably saturated groundwater-surface water flow. In ParFlow, Richards equation is discretized in space using finite differences and an implicit backward Euler scheme in time. Overland flow is modeled by solving the kinematic wave equation in a finite volume approach. ParFlow receives the incoming precipitation after canopy interception as well as the water loss from evapotranspiration from CLM3.5. In turn, ParFlow provides the hydrologic state to CLM3.5 in terms of soil moisture and matric potential.

In TSMP, the coupler OASIS3-MCT (Valcke, 2013) connects the different component models in the form of independent executables based on a Multiple Process Multiple Data (MPMD) approach. OASIS3-MCT acts as the driver initializing the models, managing the time steps and coupling frequencies, exchanging the coupling data in 2-D arrays in memory and finally terminating the simulation.

2.2 Model domain and setup

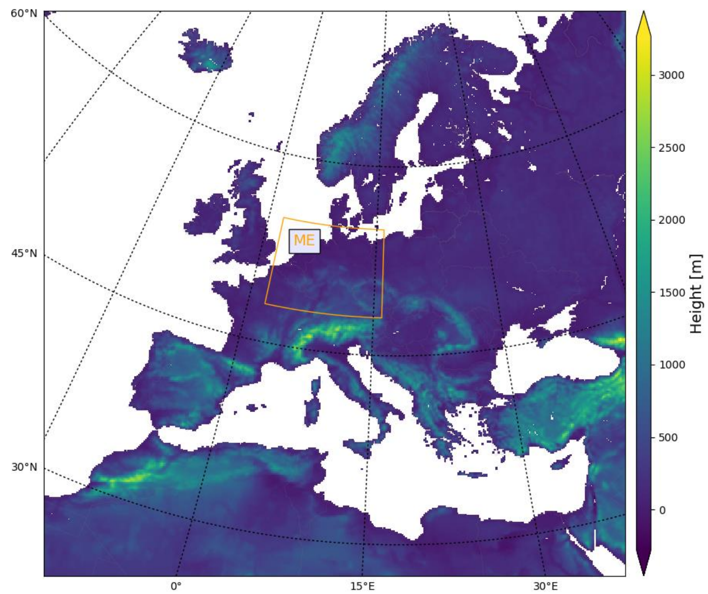

Figure 1. The European CORDEX model domain including the topographic height. The box indicates the Mid-Europe (ME) focus region of this study.

The model domain shown in figure 1 has been implemented according to the Coordinated Regional climate Downscaling Experiment (CORDEX) (Giorgi et al., 2009). The domain covers all Europe based on a rotated latitude-longitude grid with a horizontal resolution of 0.11° resulting in a resolution of approximately 12.5 km. COSMO has a vertical range of 50 km with a time step of 60 s. CLM has ten soil layers ranging 3 m into the soil, ParFlow has five extra layers covering in total 57 m depth below the land surface. The first ten layers of CLM and ParFlow are identical. In ParFlow, there is a variable vertical discretization ranging from 2cm at the land surface to more than ~10^1m toward the bottom of the aquifer based on a terrain following grid. CLM3.5 and ParFlow use a time step of 900 s, which also constitutes the coupling frequency.

Topographic slopes required by ParFlow were estimated from the USGS GTOPO30. Boundary conditions on the coast are set by a constant hydraulic pressure with a hydrostatic profile for ParFlow. The soil parameters of ParFlow model are estimated with the help of the Food and Agricultural Organization (FAO) database (Carballas et al., 1990). To achieve this fifteen types of soil are defined based on the texture information. To account for the loss of information due to spatial aggregation and anisotropy, the values of the horizontal permeability are scaled by 1000. For CLM, PFTs are obtained from the Moderate Resolution Imaging Spectroradiometer (MODIS) database (Friedl et al., 2002). The individual values for stem and leaf area index and the monthly bottom and top heights of the PFT are calculated with the global CLM surface data set. Additional details of the setup can be obtained from Furusho et al., (2019)

2.3 Setup of the probabilistic prediction system

The setup of the probabilistic prediction system is directed at the goal to provide interannual water resources predictions including droughts. The system is designed to account for the climatologic atmospheric uncertainty, since atmospheric processes are arguably not predictable at that time scale. To initialize the prediction, the terrestrial state in terms of water and energy at the end of the previous water year was applied, in this case August 2018. This state was obtained from a climatological/evaluation (EVAL) simulation starting in 1989 by Furusho et al. (2019) based on atmospheric boundary conditions from ERA-Interim (Dee et al., 2011). Then the following water year was simulated, here 2018/19, applying all previous years as atmospheric boundary conditions proposing that the predicted year is contained in the climatologic ensemble of all previous years with respect to atmospheric conditions. In this way, we are able to account for the climatologic atmospheric uncertainty without any prior assumptions. Furusho et al. (2019) analyzed the climatology starting from 1996 due to spin up effects that were detected in 1989 to 1995. Therefore only the atmospheric forcing of the water years 1996 to 2018 was applied resulting in an ensemble of 22 forcing years for 2018/19 potentially reducing the real uncertainty range.

2.4 Analyses

In the analyses, we focused on the region of Mid-Europe (ME), where the drought 2018 was pronounced. For the analysis, the data was extracted in spatially averaged, monthly mean values. The variables considered at this point are 2m air temperature, *tas* (K), precipitation, *pr* (L), and total column water storage $s_{i,j}$ (L) from the land surface to the bottom of the aquifer. The latter constitutes an integrated measure of water resources and was calculated as follows

$$s_{i,j} = \sum_{k}^{nz} sat_{i,j,k}\, por_{i,j,k}\, dz_k$$

where $sat_{i,j,k}$ is the relative saturation (-), $por_{i,j,k}$ the porosity (-) for a pixel with indices i, j, k in the lateral and vertical direction, respectively, dz_k is the extent of a vertical grid cell (L) and nz is the number of grid cells in the vertical direction. This leads to a storage estimation for every subsurface column in the model. Utilizing the monthly mean values, monthly anomalies were calculated for each pixel and then the Mid-Europe (ME) domain.

In order to evaluate the simulations, ME averaged time series for *tas* and *pr* were compared to ERA-Interim information, and *s* were compared to GRACE mascon data (Watkins et al., 2015). In the latter, the *s* anomalies were recalculated based on the time period used in the GRACE mascon data set. Interactions with the atmosphere were inspected, in particular precipitation, by subtracting the monthly precipitation values from the probabilistic prediction. In other words, every ensemble member of the year 2019 with the initial condition of the drought year 2018 was subtracted from the corresponding values of the same month of EVAL. Box plots of precipitation increments were generated for each month of the water year 2018/19 in order to identify systematic changes in monthly precipitation amounts due to the dry initial condition in the probabilistic predictions.

4 Results and discussion

While the probabilistic prediction covers all Europe, the 2018 drought was most pronounced in central, northern Europe. Therefore, in this study, we focus on Mid-Europe (ME), which is part of the PRUDENCE regions defined in Christensen and Christensen (2007).

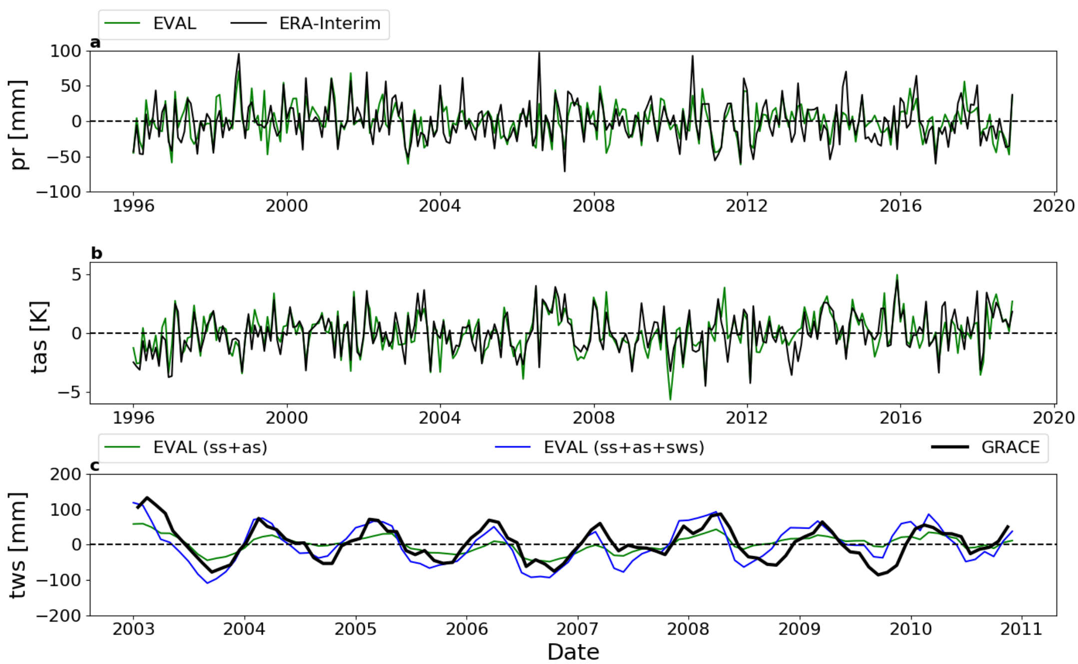

Figure 2. Anomalies calculated from ERA-Interim and the evaluation run, EVAL, from 1996 to 2018 over Mid-Europe for (a) monthly precipitation, *pr*, and (b) air temperature, *tas*. Storage anomalies *s* (c) were calculated for the entire soil column including soil water, *ss*, and aquifer, *as*,

storages (*ss* + *as*) and also surface water storage (*ss* + *as* + *sws*) based on the time period used on the GRACE mascon data set.

Figure 2 a) and b) show monthly anomalies of air temperature, *tas* and precipitation, *pr*, calculated over the subdomain ME from 1996 to 2018, respectively. The black curve shows ERA-Interim for comparison. The plots for *tas* and *pr* anomalies show that the EVAL is in good agreement with ERA-Interim, which is remarkable, because EVAL constitutes a transient simulation without any correction (e.g. nudging). In case of *s* a comparison with the GRACE mascon data was performed. In contrast to a) and b) the mean storage is calculated from 2004 to 2009 as a single value for the whole period to be comparable to the GRACE data. Additionally, we derived two different water storage anomalies for EVAL. The first anomaly consists of soil water storages, *ss*, and aquifer storage, *as*, following equation 1 covering the entire subsurface column from the land surface to the bottom of the aquifer (*ss* + *as*). The second anomaly additionally includes surface water of rivers and streams (*ss* + *as* + *sws*). There is a good agreement with GRACE in case of subsurface and surface water storage anomalies (*ss* + *as* + *sws*). In some years, there is a small phase shift in the simulated anomalies. Additionally the anomalies in the water years 2007/08 and 2009/10 were over- and underestimated, respectively. At this point, we explain these discrepancies with deviations of EVAL from real world precipitation in these years. Additionally, snow and ice, and lakes were not included in the anomalies from EVAL. The anomalies of subsurface storage (*ss* +

as) only exhibit smaller amplitudes and fewer dry anomalies, which is due to the inclusion of groundwater in the analysis.

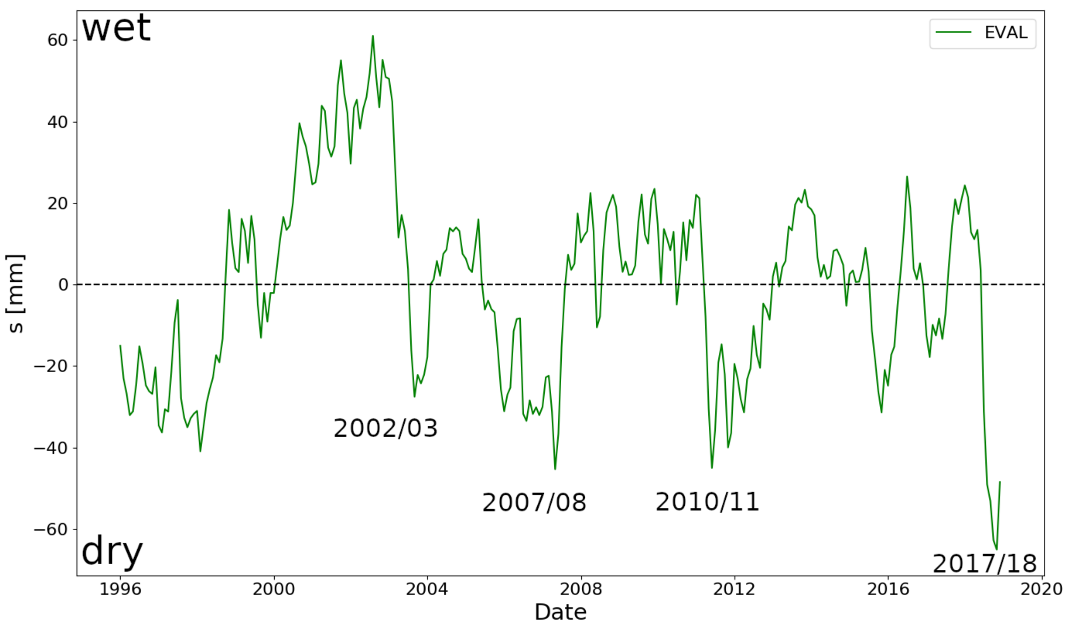

Figure 3. Time series of monthly column storage anomaly, *s*, averaged over Mid-Europe (ME) region.

Figure 3 shows the time series of monthly column storage anomalies averaged over the ME region. The major droughts of the water years 2002/03, 2007/08, 2010/11, and 2017/18 are clearly discernible. In addition, EVAL captures the transition from the extreme wet year of

2001/02, which was characterized by the massive Elbe-Danube flood, to the extreme dry year 2002/03 very well, which lends additional confidence in the forward simulations using TSMP.

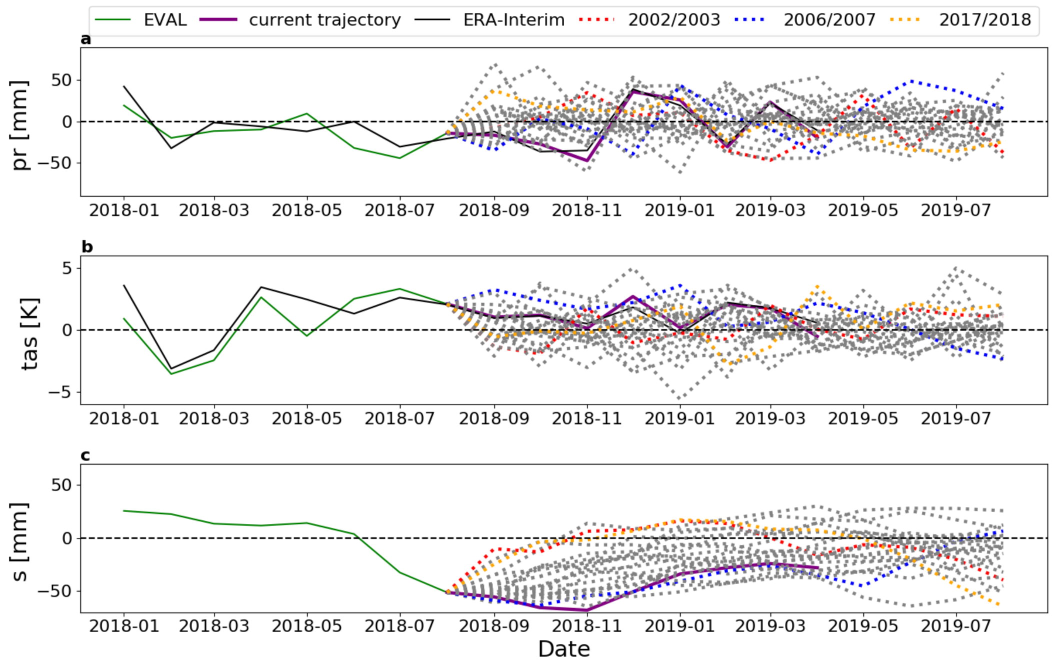

Figure 4. Plots of the period from the beginning of 2018 to August 2019 for the monthly (a) precipitation anomalies, (b) temperature anomalies and (c) the water storage anomalies. The probabilistic prediction period of the water 2018/19 includes all ensemble members in dashed lines and the current trajectory (purple solid line).

Figure 4 depicts the anomalies of *pr*, *tas* and *s* of EVAL for the period January until the end of August 2018 and the ensuing probabilistic prediction of the water year 2018/19. The heatwave is clearly visible with low precipitation (figure 4a) and high temperature anomalies (figure 4b). Over the course of the year, the influence of these two variables on the water storage, *s*, is apparent (figure 4c). The *s* anomaly changes from a wet (positive) anomaly to a strongly dry (negative) anomaly in August 2018. The hydrologic state at the end of August 2018 then served as the initial condition for the probabilistic forecast of 2019 based on the ensemble atmospheric boundary conditions of 1996/97 to 2017/18. In figure 4c, the individual ensemble members are plotted in dashed lines. We highlighted with colors dry forcing years that are 2002/03 and 2017/18, where the latter is a repetition of the extreme drought, and a wet year 2006/07. Inspection of the ensemble member 2002/03 shows that, because the end of 2002 was rather wet, this ensemble member is reducing the anomaly strongly, while the dry year 2003 increases again the negative anomaly. A repetition of 2017/18 shows similar behavior resulting in an even stronger deficit at the end of 2018/19. This is the only ensemble member that leads to an even stronger dry anomaly at the end of the simulation. 2006/07 is a wet year in the ensemble that turns the storage deficit into a positive anomaly. Most of the ensemble members reduce the dry anomaly significantly until the summer 2019, however, the majority still exhibit a significant dry anomaly at the end of the water year 20018/19. Thus, there is an increased probability that the drought continues well into the water year 2019/20. Inspecting the current trajectory (purple line in figure 4c) from the simulation using the most recent ERA-Interim boundary information (at the time of submission) the dry anomaly is increasing even beyond the ensemble emphasizing the strength of the drought 2018, which reached its peak in November 2018. While the dry anomaly decreased during the winter and spring, the current trajectory is located in the dry tail of the ensemble suggesting that there is a high probability of continuing drought conditions throughout the current water year and potentially also 2019/20.

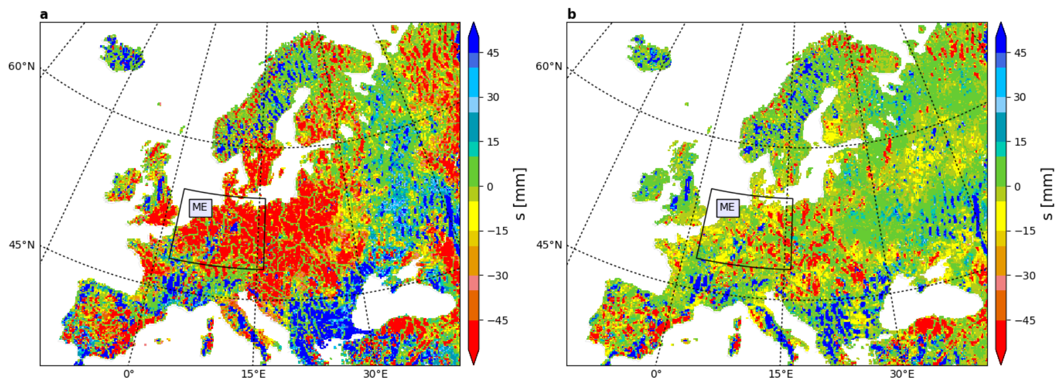

Figure 5. Water storage anomaly over the European model domain with a focus on the Mid-Europe region (ME) (a) for August 2018 and (b) the mean of all ensemble members in August 2019.

Figure 5 provides the results of the spatial analyses of the *s* anomaly over Europe. In August 2018 (figure 5a) the water deficit is significant, especially in the ME region, which is consistent with real-world observations. The ensemble mean (figure 5b) of the probabilistic prediction suggests that over large parts of ME the drought will persist at least until the end of the water year 2018/19. Figure 5 also emphasizes the strong spatial variability from the regional to the continental scale, which depends on multi-scale heterogeneity in physical parameters and fluxes especially related to evapotranspiration and precipitation. At the smallest spatial scale on the order of the resolution of the model, the anomaly patterns need to be treated with care because of the uncertainty related to local rainfall amounts in the transient coupled simulations.

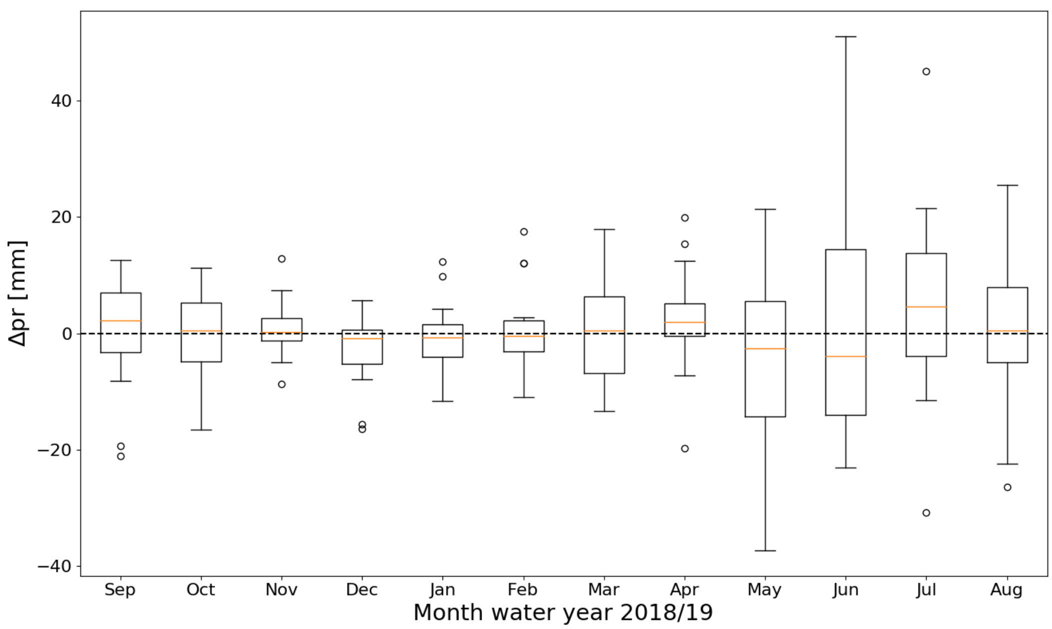

Figure 6. Boxplot of the difference of the evaluation run minus the corresponding ensemble member, Δpr, for all years. Lower to upper quartile are marked with the box, the median is indicated by the yellow line, the range of the data is indicated by the bars and the outliers are marked with circles.

The question remains, whether the extreme hydrologic drought interacted and continues to interact with atmospheric processes in the water year 2018/19. We attempted to answer the question in a rather *ad hoc* fashion at the spatial scale of the ME domain and the monthly time scale by inspecting the increments of monthly precipitation amounts from the individual ensemble members and the years of the EVAL simulation. With the help of the increments we tested the hypothesis that the extreme drought 2018 reduced precipitation amounts in the ensuing water year 2018/19. Figure 6 shows the boxplots of the increments, which do not exhibit a systematic reduction (or increase) in precipitation following the 2018 drought. The increments fluctuate around zero with increasing variance until the end of the probabilistic prediction period, which does not suggest a systematic reduction of precipitation amounts in the water year 2018/19 due to the drought 2018 at the considered space and time scale.

5 Summary and conclusions

The study proposes an interannual probabilistic prediction system of the terrestrial system from groundwater across the land surface into the atmosphere at the continental scale. Atmospheric uncertainty is accounted for by utilizing many years of historic atmospheric information as boundary conditions for the predictions. The system was applied to the water year 2018/19 based on the initial condition of the extreme drought at the end of the water year 2017/18 over the Mid--European region (ME), which is the focus of this study.

In order to verify the prediction system over ME, results from an extended evaluation simulation from 1996 to 2018 were compared to results from ERA-Interim and GRACE satellite information, which showed good agreement. While this lends confidence in the predictive skill of the applied Terrestrial Systems Modeling Platform, additional verification is required for additional variables, and different space and time scales. Further inspection of the evaluation anomalies showed that 2018 was the strongest drought in terms subsurface water storage since 1996. The results from the probabilistic prediction indicated that there is a high probability of a continuing water deficit at the end of August 2019 due to memory effects of the drought 2018 of the subsurface-land surface system. The current trajectory of the water storage anomaly for 2018/19 suggests that the strong drought may persist also into 2019/20. Currently, 22 years of historic atmospheric forcing has been applied in an attempt to capture the atmospheric uncertainty, which is probably not enough. Additional years will be added to assess the robustness of the approach. An increment analysis of precipitation amounts suggested that the 2018 drought did not influence precipitation in the water year 2018/2019 in an average sense over ME. However the analysis was limited; in future, more work is needed to interrogate subsurface-land and surface-atmosphere feedbacks across multiple space and time scales, and variables. The prediction system has the potential to provide continues, quasi-operational probabilistic predictions over the course of a water year given enough computational and data storage resources, which are significant. Additionally, the current trajectory can be continuously updated with incoming atmospheric re-analyses in order to provide continues information on the current state of the terrestrial system. We provide this information and the data sets of this study at https://datapub.fz-juelich.de/slts/prob_cordex/. Note, in this study, the system was applied in the context of water scarcity. In the future, the potential for probabilistic flood forecasting will be explored as well.

Acknowledgments

The authors gratefully acknowledge the computing time granted through JARA-HPC and the VSR commission on the supercomputer JUWELS at Research Centre Jülich through compute time projects cjibg35.

The work described in this paper has received funding from the Initiative and Networking Fund of the Helmholtz Association (HGF) through the project “Advanced Earth System Modelling

Capacity (ESM)". The content of the paper is the sole responsibility of the author(s) and it does not represent the opinion of the Helmholtz Association, and the Helmholtz Association is not responsible for any use that might be made of the information contained. The data is made available at https://datapub.fz-juelich.de/slts/prob_cordex/.

References

Ashby, S. F., & Falgout, R. D. (1996). A Parallel Multigrid Preconditioned Conjugate Gradient Algorithm for Groundwater Flow Simulations. Nuclear Science and Engineering, 124(1), 145–159. https://doi.org/10.13182/NSE96-A24230

Baldauf, M., Seifert, A., Foerstner, J., Majewski, D., Raschendorfer, M., & Reinhardt, T. (2011). Operational Convective-Scale Numerical Weather Prediction with the COSMO Model: Description and Sensitivities. MONTHLY WEATHER REVIEW, 139(12), 3887–3905. https://doi.org/10.1175/MWR-D-10-05013.1

Carballas, T., Macias, F., Diaz-Fierros, F., Carballas, M., & Fernandez-Urrutia, J. A. (1990). FAO-UNESCO soil map of the world. Revised legend. Informes Sobre Recursos Mundiales de Suelos (FAO).

Christensen, J. H., & Christensen, O. B. (2007). A summary of the PRUDENCE model projections of changes in European climate by the end of this century. Climatic Change, 81(SUPPL. 1), 7–30. https://doi.org/10.1007/s10584-006-9210-7

Dee, D. P., Uppala, S. M., Simmons, A. J., Berrisford, P., Poli, P., Kobayashi, S., et al. (2011). The ERA-Interim reanalysis: Configuration and performance of the data assimilation system. Quarterly Journal of the Royal Meteorological Society, 137(656), 553–597. https://doi.org/10.1002/qj.828

Dirmeyer, P. A. (2000). Using a global soil wetness dataset to improve seasonal climate simulation. Journal of Climate, 13(16), 2900–2922. https://doi.org/10.1175/1520-0442(2000)013<2900:UAGSWD>2.0.CO;2

Friedl, M. A., McIver, D. K., Hodges, J. C. F., Zhang, X. Y., Muchoney, D., Strahler, A. H., et al. (2002). Global land cover mapping from MODIS: Algorithms and early results. Remote Sensing of Environment. https://doi.org/10.1016/S0034-4257(02)00078-0

Furusho, C., Goergen, K., Kulkarni, K., Keune, J., & Kollet, S. (2019). Pan-European groundwater to atmosphere terrestrial systems climatology from a physically consistent simulation. https://doi.org/10.31223/OSF.IO/8VHG5

Gasper, F., Goergen, K., Shrestha, P., Sulis, M., Rihani, J., Geimer, M., & Kollet, S. (2014). Implementation and scaling of the fully coupled Terrestrial Systems Modeling Platform (TerrSysMP v1.0) in a massively parallel supercomputing environment - a case study on JUQUEEN (IBM Blue Gene/Q). GEOSCIENTIFIC MODEL DEVELOPMENT, 7(5), 2531–2543. https://doi.org/10.5194/gmd-7-2531-2014

Giorgi, F., Jones, C., Asrar, G. R., & others. (2009). Addressing climate information needs at the regional level: the CORDEX framework. World Meteorological Organization (WMO) Bulletin, 58(3), 175.

Hao, Z., AghaKouchak, A., Nakhjiri, N., & Farahmand, A. (2014). Global integrated drought monitoring and prediction system. Scientific Data, 1, 140001. https://doi.org/10.1038/sdata.2014.1

Hirschi, M., Seneviratne, S. I., Alexandrov, V., Boberg, F., Boroneant, C., Christensen, O. B., et al. (2011). Observational evidence for soil-moisture impact on hot extremes in southeastern Europe. Nature Geoscience, 4(1), 17–21. https://doi.org/10.1038/ngeo1032

Hosseini-Moghari, S. M., & Araghinejad, S. (2015). Monthly and seasonal drought forecasting using statistical neural networks. Environmental Earth Sciences, 74(1), 397–412. https://doi.org/10.1007/s12665-015-4047-x

Jones, J. E., & Woodward, C. S. (2001). Newton-Krylov-multigrid solvers for large-scale, highly heterogeneous, variably saturated flow problems. Advances in Water Resources. https://doi.org/10.1016/S0309-1708(00)00075-0

Keune, J., Gasper, F., Goergen, K., Hense, A., Shrestha, P., Sulis, M., & Kollet, S. (2016). Studying the influence of groundwater representations on land surface-atmosphere feedbacks during the European heat wave in 2003. JOURNAL OF GEOPHYSICAL RESEARCH-ATMOSPHERES, 121(22), 13301–13325. https://doi.org/10.1002/2016JD025426

Keune, J., Sulis, M., Kollet, S., Siebert, S., & Wada, Y. (2018). Human Water Use Impacts on the Strength of the Continental Sink for Atmospheric Water. GEOPHYSICAL RESEARCH LETTERS, 45(9), 4068–4076. https://doi.org/10.1029/2018GL077621

Kollet, S. J., & Maxwell, R. M. (2006). Integrated surface-groundwater flow modeling: A free-surface overland flow boundary condition in a parallel groundwater flow model. ADVANCES IN WATER RESOURCES, 29(7), 945–958. https://doi.org/10.1016/j.advwatres.2005.08.006

Lo, M. H., & Famiglietti, J. S. (2010). Effect of water table dynamics on land surface hydrologic memory. Journal of Geophysical Research Atmospheres, 115(22), 1–12. https://doi.org/10.1029/2010JD014191

Madadgar, S., & Moradkhani, H. (2013). A Bayesian Framework for Probabilistic Seasonal Drought Forecasting. Journal of Hydrometeorology, 14(6), 1685–1705. https://doi.org/10.1175/jhm-d-13-010.1

Maxwell, R. M. (2013). A terrain-following grid transform and preconditioner for parallel, large-scale, integrated hydrologic modeling. Advances in Water Resources, 53, 109–117. https://doi.org/10.1016/j.advwatres.2012.10.001

Maxwell, R. M., Chow, F. K., & Kollet, S. J. (2007). The groundwater–land-surface–atmosphere connection: Soil moisture effects on the atmospheric boundary layer in fully-coupled simulations. Advances in Water Resources, 30(12), 2447–2466. https://doi.org/10.1016/J.ADVWATRES.2007.05.018

Miguez-Macho, G., & Fan, Y. (2012). The role of groundwater in the Amazon water cycle: 1. Influence on seasonal streamflow, flooding and wetlands. Journal of Geophysical Research: Atmospheres, 117(D15), n/a-n/a. https://doi.org/10.1029/2012JD017539

Miralles, D. G., Gentine, P., Seneviratne, S. I., & Teuling, A. J. (2019). Land–atmospheric feedbacks during droughts and heatwaves: state of the science and current challenges. Annals of the New York Academy of Sciences, 1436(1), 19–35. https://doi.org/10.1111/nyas.13912

Mishra, A. K., & Desai, V. R. (2005). Drought forecasting using stochastic models. Stochastic Environmental Research and Risk Assessment, 19(5), 326–339. https://doi.org/10.1007/s00477-005-0238-4

Oleson, K. W., Dai, Y., Bonan, G. B., Bosilovich, ., Dickinson, R. E., Dirmeyer, P. A., et al. (2004). Technical Description of the Community Land Model (CLM). NCAR Technical Note, NCAR/TN-46, 186. https://doi.org/10.5065/D6N877R0

Oleson, K. W., Niu, G. Y., Yang, Z. L., Lawrence, D. M., Thornton, P. E., Lawrence, P. J., et al. (2008). Improvements to the community land model and their impact on the hydrological cycle. Journal of Geophysical Research: Biogeosciences, 113(1). https://doi.org/10.1029/2007JG000563

Rhee, J., & Im, J. (2017). Meteorological drought forecasting for ungauged areas based on machine learning: Using long-range climate forecast and remote sensing data. Agricultural and Forest Meteorology. https://doi.org/10.1016/j.agrformet.2017.02.011

Seneviratne, S. I., Corti, T., Davin, E. L., Hirschi, M., Jaeger, E. B., Lehner, I., et al. (2010). Investigating soil moisture–climate interactions in a changing climate: A review. Earth-Science Reviews, 99(3–4), 125–161. https://doi.org/10.1016/J.EARSCIREV.2010.02.004

Sheffield, J., Wood, E. F., Chaney, N., Guan, K., Sadri, S., Yuan, X., et al. (2013). A Drought Monitoring and Forecasting System for Sub-Sahara African Water Resources and Food Security. Bulletin of the American Meteorological Society, 95(6), 861–882. https://doi.org/10.1175/bams-d-12-00124.1

Shrestha, P., Sulis, M., Masbou, M., Kollet, S., & Simmer, C. (2014). A Scale-Consistent Terrestrial Systems Modeling Platform Based on COSMO, CLM, and ParFlow.

MONTHLY WEATHER REVIEW, 142(9), 3466–3483. https://doi.org/10.1175/MWR-D-14-00029.1

Valcke, S. (2013). The OASIS3 coupler: a European climate modelling community software. Geoscientific Model Development, 6(2), 373–388. https://doi.org/10.5194/gmd-6-373-2013

Walko, R. L., Band, L. E., Baron, J., Kittel, T. G. F., Lammers, R., Lee, T. J., et al. (2000). Coupled Atmosphere–Biophysics–Hydrology Models for Environmental Modeling. Journal of Applied Meteorology, 39(6), 931–944. https://doi.org/10.1175/1520-0450(2000)039<0931:CABHMF>2.0.CO;2

Watkins, M. M., Wiese, D. N., Yuan, D.-N., Boening, C., & Landerer, F. W. (2015). Improved methods for observing Earth's time variable mass distribution with GRACE using spherical cap mascons. Journal of Geophysical Research: Solid Earth, 120(4), 2648–2671. https://doi.org/10.1002/2014JB011547

York, J. P., Person, M., Gutowski, W. J., & Winter, T. C. (2002). Putting aquifers into atmospheric simulation models: an example from the Mill Creek Watershed, northeastern Kansas. Advances in Water Resources, 25(2), 221–238. https://doi.org/10.1016/S0309-1708(01)00021-5

Yuan, X., & Wood, E. F. (2013). Multimodel seasonal forecasting of global drought onset. Geophysical Research Letters, 40(18), 4900–4905. https://doi.org/10.1002/grl.50949

Yuan, X., Wood, E. F., Chaney, N. W., Sheffield, J., Kam, J., Liang, M., & Guan, K. (2013). Probabilistic Seasonal Forecasting of African Drought by Dynamical Models. Journal of Hydrometeorology, 14(6), 1706–1720. https://doi.org/10.1175/JHM-D-13-054.1

Zink, M., Pommerencke, J., Kumar, R., Thober, S., Samaniego, L., & Marx, A. (2016). The German Drought Monitor. Environmental Research Letters, 17, 5625.